First publ. in: Chemistry of Materials 15 (2003), pp. 3586-3593

Redox Behavior of Nanostructured Molybdenum Oxide−Mesoporous Silica Hybrid Materials

V. Hornebecq,[†,§] Y. Mastai,[†] M. Antonietti,[†] and S. Polarz*[,‡]

Max-Planck Institute of Colloids and Interfaces, Research Campus Golm, 14424 Potsdam, Germany, and Department of Inorganic Chemistry, Nanostructured Materials Group, Ruhr-University Bochum, 44780 Bochum, Germany

Encapsulation of molybdenum oxide MoO_3 into ordered mesoporous silica materials is demonstrated using different synthetic routes. Either supramolecular polyoxometalates of the "Müller type" or Na_2MoO_4 were used as precursors. Molybdenum oxide (MoO_3)−silica hybrid materials were characterized using nitrogen-sorption experiments, transmission electron microscopy, small-angle X-ray scattering, and infrared spectroscopy. Under reducing conditions, the hybrid materials undergo an electrochromic transition from colorless or slightly yellow to blue without any leaching of Mo species from the materials. The electrochromic response, which is fully reversible, is caused by a transition from Mo^{VI} to a mixed valence Mo^{VI}/Mo^{V} molybdenum oxide encapsulated in the pores. The reduction process was studied using in situ electron spin resonance (ESR) and UV/vis absorption measurements. Materials of different pore sizes were used, and it was found that pore size effects the kinetics of the reaction.

Introduction

Nanostructures and nanostructured materials are becoming increasingly important in various fields such as chemistry, materials science, chemical engineering, and physics. Nanostructures are fascinating because of their unique properties (optical, electrical, magnetic, etc.) often related to, or caused by, quantum size effects. It is further believed that once methods for the preparation of single nanocomponents are established, rational designs will be found to combine these components to materials that have synergistic properties.[1−3]

Ordered mesoporous silica materials[4−7] can be seen as raw models for nanostructured materials as well as nanoporous materials[8] for two reasons. First, ordered mesoporous silica materials are truly nanostructured. Accessible pore morphologies range from spherical voids,[9,10] cylindrical voids in a hexagonal alignment,[4,5,11,12] curved and interconnected voids as in the gyroid phase,[13,14] to less ordered materials possessing a "worm-type" pore morphology. Pore sizes range mainly from 1 to 10 nm,[15] and in the case of appropriate templates pores up to 80 nm[16,17] may be obtained. If one even takes opals and inverted opals into account, still larger pores are accessible. Second, these kinds of voids have been proven useful for the controlled synthesis of other nanostructures such as metal- or semiconductor colloids (the "nanoreactor" approach).[18] The size and shape of the resulting colloids or nanoparticles can be controlled by the size and shape of the confinement.[19] This new type of chemistry, where the formation of colloids and nanoparticles is guided by spatial confinements, was also named "nanochemistry".[20,21]

One of the unique features of transition metals in general and molybdenum oxide compounds in particular is the reversible character of redox processes between two oxidation states. As in the case of molybdenum (redox pair Mo^{VI}/Mo^{V}), this redox process is often guided by a change in the optical properties, a phenomenon

* To whom correspondence should be addressed. E-mail: sebastian.polarz@ruhr-uni-bochum.de.
† Max-Planck Institute of Colloids and Interfaces.
‡ Ruhr-University Bochum.
§ V. Hornebecq and S. Polarz contributed equally to this work. E-mail: Virginie.Hornebecq@mpikg-golm.mpg.de.

(1) Whitesides, G. *Technol. Rev.* **1998**, *101*, 84.
(2) Whitesides, G. M. *Sci. Am.* **2001**, *285*, 78.
(3) Whitesides, G. M.; Love, J. C. *Sci. Am.* **2001**, Sept., 33.
(4) Kresge, C. T.; Leonowicz, M.; Roth, W. J.; Vartuli, J. C.; Beck, J. S. *Nature* **1992**, *359*, 710.
(5) Beck, J. S.; Vartuli, J. C.; Roth, W. J.; Leonowicz, M. E.; Kresge, C. T.; Schmitt, K. D.; Chu, C. T.; Olson, D. H.; Sheppard, E. W.; McCullen, S. B.; Higgins, J. B.; Schlenker, J. L. *J. Am. Chem. Soc.* **1992**, *114*, 10834.
(6) Ciesla, U.; Schüth, F. *Microporous Mesoporous Mater.* **1999**, *27*, 131.
(7) Polarz, S. *Silica Organic Hybrid Materials*; American Scientific Publishers: 2002.
(8) Polarz, S.; Smarsly, B. *J. Nanosci. Nanotechnol.* **2003**, *2*, 581.
(9) Tolbert, S. H.; Schaffer, T. E.; Feng, J. L.; Hansma, P. K.; Stucky, G. D. *Chem. Mater.* **1997**, *9*, 1962.
(10) Huo, Q.; Leon, R.; Petroff, P. M.; Stucky, G. D. *Science* **1995**, *268*, 1324.
(11) Zhao, D.; Huo, Q.; Feng, J.; Chmelka, B. F.; Stucky, G. D. *J. Am. Chem. Soc.* **1998**, *120*, 6024.
(12) Zhao, D.; Feng, J.; Huo, Q.; Melosh, N.; Fredrickson, G. H.; Chmelka, B. F.; Stucky, G. D. *Science* **1998**, *279*, 548.
(13) Alfredsson, V.; Anderson, M. W. *Chem. Mater.* **1996**, *8*, 1141.
(14) Anderson, M. W. *Zeolites* **1997**, *19*, 220.
(15) Smarsly, B.; Polarz, S.; Antonietti, M. *J. Phys. Chem. B* **2001**, *105*, 10473.
(16) Krämer, E.; Förster, S.; Göltner, C.; Antonietti, M. *Langmuir* **1998**, *14*, 2027.
(17) Hentze, H. P.; Krämer, E.; Berton, B.; Förster, S.; Antonietti, M. *Macromolecules* **1999**, *32*, 5803.
(18) Weller, H. *Angew. Chem., Int. Ed. Engl.* **1993**, *32*, 41.
(19) Bronstein, L. M.; Polarz, S.; Smarsly, B.; Antonietti, M. *Adv. Mater.* **2001**, *13*, 1333.
(20) Ozin, G. A. *Adv. Mater.* **1992**, *4*, 612.
(21) Ozin, G. A.; Chomski, E.; Khushalani, D.; Maclachlan, M. J. *Curr. Opin. Colloid Interface Sci.* **1998**, *3*, 181.

known as electrochromism.[22−25] However, the optical response of an electrochromic material may be utilized to sense the presence of reduction or oxidation agents. This field is to the best of our knowledge rather unexplored, and polyoxometalate−silica hybrid materials have not been used for this purpose. Many materials of this type, which can be seen as a subgroup of so-called intelligent materials,[26] have polymers as their active species but also some materials based on transition metals have been published.[27−33] From this point of view, nanostructures of molybdenum oxide in the form of MoO_3 or as polyoxometalate clusters as in the famous Müller-type compounds[34−36] are interesting target structures for materials with redox sensing or electrochromic properties. Furthermore, porous materials hosting molybdenum oxide species are promising for catalysis.

In the present study, we focus on the preparation of porous molybdenum oxide−silica hybrid materials using different ways of synthesis and precursors. Ordered mesoporous silica materials were chosen as the support for the redox-active molybdenum oxide species. This approach has several advantages. The ordered mesoporous network provides very well defined transport systems for the redox agents. The control over the properties of the "transport system" should have a significant influence on the performance of the materials. Furthermore, the spatial confinement of the silica pores enables production of nanosized molybdenum oxide. By combination of nitrogen sorption measurements, electronic microscopy, X-ray techniques, infrared spectroscopy, and optical absorption methods, samples were characterized and their redox properties were investigated.

Experimental Section

As mentioned in the Introduction, two different ways of synthesis were used to prepare molybdenum oxide−silica hybrid materials (Figure 1). In route 1, supramolecular polyoxometalates of the Müller type act as templates and precursors for MoO_3 simultaneously.[37,38] In route 2, ordered mesoporous silica materials are derived by amphiphilic organization

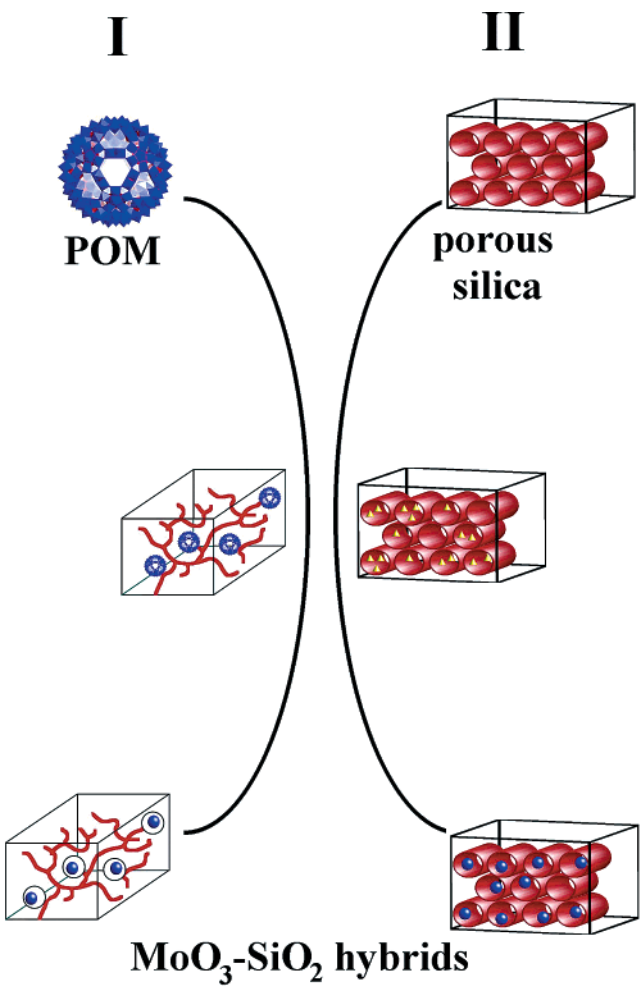

Figure 1. Schematic representation of the two nanochemical routes toward porous MoO_3−silica composite materials. Supramolecular polyoxometalates of the Mueller type are used as templates for the creation of pores first and react then under the confinement of their self-created pores to MoO_3, as depicted in route I. Then, polyoxometalate-containing pores are interconnected by smaller pores created by cyclodextrins as templates. On the other hand (route II), ordered mesoporous silica materials can be prefabricated and then filled with appropriate sources for MoO_3.

of surfactants or block copolymers[39,40] as templates and are infiltrated with MoO_3 precursors.

Preparation of Molybdenum Oxide−Silica Hybrids (Route I) S_1. A giant polyoxometalate (POM) of the Müller type[35,41] $[Mo_{132}O_{372}(CH_3COO)_{30}(H_2O)_{72}]^{42-}$ (denoted Mo_{132}) was used as the source for MoO_3.[34,35] Earlier work has proven[37] that this cluster is fully compatible under silica sol−gel conditions and that this cluster creates its own pockets in an otherwise dense silica matrix. It was also shown that even when chemical reactions are performed with these clusters, the amount of molybdenum units in every pore stays constant. To obtain access to these pores, a second, bicontinuous pore system possessing much smaller pores was created, chosen in a way that the molybdenum fragments cannot leave the big pores, preserving the amount of molybdenum per POM pore. This additional "transport" porosity of size 1.5 nm was achieved by employing β-MCD (a statistically methylated cyclodextrin) as a template.[42] In particular, 100 mg of Mo_{132}

(22) Mortimer, R. J. *Chem. Soc. Rev.* **1997**, *26*, 147.
(23) Granqvist, C. G. *Appl. Phys. A: Mater. Sci. Process.* **1993**, *57*, 3.
(24) Lampert, C. M. *Sol. Energy Mater.* **1984**, *11*, 1.
(25) Dautremontsmith, W. C. *Displays* **1982**, *3*, 3.
(26) Baughman, R. H. *Makromol. Chem.-Macromol. Symp.* **1991**, *51*, 193.
(27) Ozin, G. A.; Mamak, M. *Abstr. Pap. Am. Chem. Soc.* **2000**, *219*, 347-INOR.
(28) Perez, E. F.; Neto, G. D.; Tanaka, A. A.; Kubota, L. T. *Electroanalysis* **1998**, *10*, 111.
(29) Tschope, A.; Schaadt, D.; Birringer, R.; Ying, J. Y. *Nanostruct. Mater.* **1997**, *9*, 423.
(30) Bychkov, E.; Bruns, M.; Geckle, U.; Hoffmann, W.; Schlesinger, R.; Ache, H. J. *Solid State Ionics* **1994**, *74*, 165.
(31) Tieman, R. S.; Igo, D. H.; Heineman, W. R.; Johnson, J.; Seguin, R. *Sens. Actuators, B* **1991**, *5*, 121.
(32) Wright, J. D. *Inst. Phys. Conf. Ser.* **1990**, 333.
(33) Liu, S. G.; Echegoyen, L. *Abstr. Pap. Am. Chem. Soc.* **2001**, *222*, 553-ORGN.
(34) Müller, A.; Krickemeyer, E.; Bögge, H.; Schmidtmann, M.; Peters, F. *Angew. Chem.* **1998**, *110*, 3567.
(35) Müller, A.; Polarz, S.; Das, S. K.; Krickemeyer, E.; Bögge, H.; Schmidtmann, M.; Hauptfleisch, B. *Angew. Chem.* **1999**, *111*, 3439.
(36) Müller, A.; Shah, S. Q. N.; Bögge, H.; Schmidtmann, M. *Nature* **1999**, *397*, 48.
(37) Polarz, S.; Smarsly, B.; Göltner, C.; Antonietti, M. *Adv. Mater.* **2000**, *12*, 1503.
(38) Mastai, Y.; Polarz, S.; Antonietti, M. *Adv. Funct. Mater.* **2002**, *12*, 197.
(39) Attard, G. S.; Göltner, C. G.; Corker, L. M.; Henke, S.; Templer, R. H. *Angew. Chem.* **1997**, *109*, 1372.
(40) Göltner, C.; Cölfen, H.; Antonietti, M. *Chem. Unserer Zeit* **1999**, *33*, 200.
(41) Müller, A.; Krickemeyer, E.; Bögge, H.; Schmidtmann, M.; Beugholt, C.; Kögerler, P.; Lu, C. *Angew. Chem.* **1998**, *110*, 1278.

was dissolved in 1 g of aqueous HCl (pH = 2.5), 0.25 g of β-MCD was added, and 2 g of TMOS was hydrolyzed under strong stirring. After homogenization the dark brown gels are aged at RT for 1 week. During this time shrinkage up to 50% of the volume occurs. The brown silica monoliths prepared as described still contain the Mo_{132} cluster and β-MCD in the pores. The CD molecules are removed by calcination at 550 °C for 5h under air, and the color of the monoliths changes to pale-yellow and is still transparent. These materials were denoted as MoO_3−silica hybrid S_1.

Preparation of Mesoporous Silicas (Route II). Mesoporous silica materials were prepared according to the nanocasting procedure[43] developed recently by Goeltner et al.[37,38] In this materials synthesis, lyotropic phases derived by amphiphilic molecules in water are used as template structures and transcribed into an ordered mesoporous material.[43] Ideally, a 1:1 replica is obtained. Several types of templates can be used to prepare mesoporous silica materials offering different pore sizes and morphologies.[43]

The lyotropic phases of nonionic *n*-alkyl-poly(ethylene oxide) surfactants (denoted C_xE_y) and block copolymers consisting of a hydrophobic polystyrene block and a hydrophilic poly(ethylene oxide) block (denoted SE_{xy}) are used as templates in the current work.[15]

Porous silica materials are prepared as follows: The amphiphile (2 g) is dissolved in tetramethyl orthosilane (TMOS) (4 g), and aqueous HCl (pH = 2) (2 g) is added. After homogenization, the evolving methanol is removed in vacuum and the resulting gel is aged for 24 h at 60 °C. Finally, the templates are removed via calcination performed in air at 550 °C for 5 h in a tubular oven.

Preparation of Molybdenum Oxide Containing Materials $S_{2/3}$. Samples denoted S_2 were prepared in the following way: The SE_{3030}−silica monoliths[15] were impregnated with the "Müller-clusters" Mo_{132} as the source for molybdenum. Materials with different sizes of pores D_p = 3 nm ($C_{18}E_{20}$−silica), 4.5 nm (SE_{1010}−silica), and 9.5 nm (SE_{3030}−silica) were used.[15] A solution of Mo_{132} (100 mg/mL H_2O) was prepared and the silica monoliths were put into this solution. The impregnation time was 24 h; afterward, the monoliths were washed with water. Due to the strong color of the Mo_{132} compound, it is very easy to judge qualitatively about the success of infiltration. Afterward, the samples were dried at RT for 2 days in air. The samples with 3 and 4.5 nm appeared to be colorless after the washing procedure, indicating that the Mo_{132} cluster could not penetrate the pore system. Mo_{132} itself has a size of about 3.5 nm as determined by single X-ray analysis.[44] The radius in water due to an adsorbed shell of water is supposedly larger. The SE_{3030}−silica with its 9.5-nm pores was on the other hand completely infiltrated; the silica monoliths had the deep brown color originating from Mo_{132}. These findings nicely underline the size sieving effects of mesoporous silica. The transformation of the Mo_{132} clusters to MoO_3 was performed by calcination in air for 2 h at 550 °C. During this process the color of the samples changed from deep brown to colorless (white).

Samples denoted S_3 were prepared in the following way. The SE3030−silica monoliths were impregnated with a Na_2MoO_4 1 M solution for 48 h; then HCl was added to induce the precipitation of the molybdenum hydrate. After 48 h, the silica materials were washed with water and sonicated to remove MoO_3 precipitates outside the pore system. The materials were then dried at 60 °C and calcined in a tubular oven at 500 °C for 10 h in an oxygen atmosphere.

Characterization Methods. TEM images were acquired on a Zeiss EM 912Ω at an acceleration voltage of 120 kV. Samples were ground in a ball mill and suspended in acetone. One droplet of the suspension was applied to a 400-mesh carbon-coated copper grid and left to dry in air. Nitrogen sorption measurements were recorded with a Micrometrics Gemini instrument. The samples for the adsorption measurements were dried under vacuum at 373 K for 24 h. Small-angle X-ray scattering (SAXS) measurements were conducted with a Nonius rotating anode (P = 4 kW, Cu Kα) and an image-plate detector system. With the detector placed at a distance of 40 cm from the sample, a scattering vector range from s = 0.05−1.6 nm^{-1} was accessible. The samples were irradiated for 18 h to reduce the noise level and to obtain a sufficiently high scattering intensity. 2D diffraction patterns were transformed into a 1D radial average of the scattering intensity. WAXS patterns were collected on an Enraf Nonius FR590 diffractometer. IR spectra were recorded on a Biorad FTS 600 FTIR spectrometer; ground materials were used for the analysis. ESR measurements were performed using a Bruker EMX spectrometer in the X-band (9.5 GHz). Diffuse reflection spectroscopy (DRS) measurements were carried out on a Jasco V-570 spectrophotometer equipped with an integrating sphere. Spectra were recorded at room temperature, from 850 to 350 nm with a scanning speed of 200 nm/min. $MgCO_3$ was used as a reference. Bulk silica powder was used as a comparison.

Results and Discussion

At first, we investigated the materials impregnation and formation of MoO_3 inside the pores before the reduction of this MoO_3 is studied.

Characterization of S_1 Materials. MoO_3 inside pores forms by an oxidation process from the reduced polyoxomolybdate Mo_{132} cluster. This if of course totally expected when Mo_{132} is calcined in an oxygen atmosphere. However, to ensure that MoO_3 is indeed formed, we compared UV/vis reflection spectra of the resulting S_1−MoO_3−silica materials directly to bulk crystalline MoO_3, which showed the same spectral features. Wide-angle X-ray scattering analysis indicates (patterns not shown) that amorphous MoO_3 is obtained. The scattering pattern just shows the broad reflex for amorphous silica at 2θ = 0.4 rad but no additional reflexes. The materials exhibit now a total surface area of 200 m^2/g, as determined by nitrogen sorption, which originates from the CD molecules as templates. However, due to the disordered pore system and the small pore size (1.5 nm), TEM characterization showed no particular features other than this disordered pore structure.

Characterization of $S_{2/3}$ Materials. The mesoporous silica materials were characterized first by nitrogen sorption analysis. The SE_{3030}−silica prior to infiltration presents a steep slope at low relative pressure, suggesting that the isotherm is not strictly of type IV (characteristic of mesoporous materials); a superposition of isotherms of type I and IV must be considered, indicating the presence of micropores (diameter < 2 nm) as also earlier found by Göltner et al.[15,45] The total surface area (BET) is 550 m^2/g and the pore-size distribution (DFT) has a maximum at 9.5 nm.

S_2 Materials. The volume of a 9.5-nm pore is ca. 450 nm^3 while a Mo_{132} cluster occupies approximately 35 nm^3 of space. In other words, a SE_{3030} pore theoretically provides space for a maximum of 12 Mo_{132} clusters. The mesoporous SE3030−silica materials containing Mo_{132} clusters have been investigated by nitrogen-sorption analysis, TEM, and X-ray analysis. The content of Mo_{132}

(42) Polarz, S.; Smarsly, B.; Bronstein, L.; Antonietti, M. *Angew. Chem., Int. Ed.* **2001**, *40*, 4417.
(43) Polarz, S.; Antonietti, M. *Chem. Commun.* **2002**, 2593.
(44) Muller, A.; Polarz, S.; Das, S. K.; Krickemeyer, E.; Bogge, H.; Schmidtmann, M.; Hauptfleisch, B. *Angew. Chem., Int. Ed.* **1999**, *38*, 3241.
(45) Göltner, C. G.; Smarsly, B.; Berton, B.; Antonietti, M. *Chem. Mater.* **2001**, *13*, 1617.

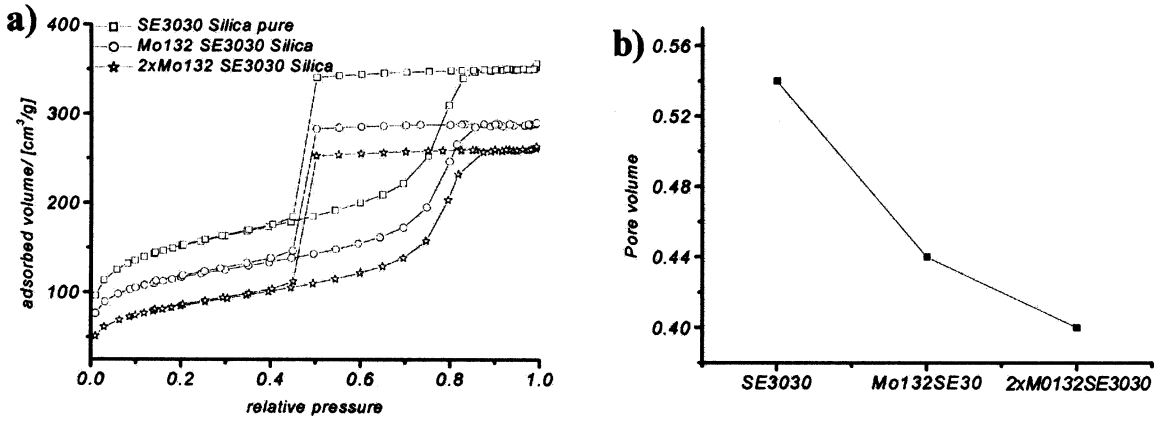

Figure 2. Nitrogen sorption isotherm (a) and evolution of pore volume (b) for MO−silica hybrid material (S_3) prior to calcination. The graph shows how the pores can be succeedingly filled with supramolecular polyoxometalates and how hence the total amount of Mo atoms per pore can be controlled.

in the porous silica can be increased by repeating the infiltration process for a second time ($2 \times Mo_{132}$).

It is seen from the recorded isotherms (Figure 2a) that the mesopore system is not blocked by the deposition of Mo_{132} clusters. The isotherms (adsorption and desorption) are practically identical but the whole isotherm is shifted to lower values for the adsorbed volume. As taken from the isotherms, the pore-size distribution shows a maximum at 9.5 nm for all three samples, which indicates that the average pore size itself is not modified by the adsorption of the clusters.

However, these findings are somewhat astonishing because one might expect an alteration in the isotherm shape as well, not just a change in the total adsorbed volume. There are two possible explanations for the observed phenomenon. It could be that the Mo_{132} blocks the pore entrance of micropores, therefore decreasing the micropore volume. It should be noted that the adsorbed volume correlating to the capillary condensation step and therefore to the mesopore volume does not change. Changes are mainly registered in the micropore region of the isotherm. This interpretation seems to be partially supported by the TEM images (Figure 3), which indicate that the Mo_{132} clusters mainly are located near the pore wall. However, we can also not exclude that small molybdate species originating from early, partial decomposition of the Mo_{132} clusters specifically bind to the micropores and therefore block them.

The samples were further investigated by TEM. The typical pore architecture for SE3030−silica is seen on all images. The imaging contrast of the samples seems to be higher than that in the corresponding bare SE3030−silica material at some places and we interpret this as a result of the infiltration with the Mo_{132} clusters. Interestingly, the clusters seem not to be homogeneously distributed throughout the material. At higher magnifications it is seen (Figure 3a, indicated by an arrow) that dark spots are located inside the pores. These spots appear to be near to the pore wall in all cases, and the diameter of a single spot can be estimated to be 3−4 nm. It is reasonable to assume that these are actually the spherical Mo_{132} clusters that are deposited in the porous framework of SE3030−silica. However, neither sorption analysis nor TEM are able to tell what exactly is infiltrated. SAXS investigations support the assumption that indeed Mo_{132} clusters are guests inside the mesopores.

The scattering curve of the Mo_{132}−SE_{3030}−silica hybrid material seems to be a superposition of two scattering patterns, the SE_{3030}−silica pattern and the form-factor scattering of Mo_{132} (Figure 3b). The scattering maximum at $s = 0.07$ nm^{-1} is typical for the mesostructure ($\approx d$ spacing) of ordered mesoporous SE3030−silica samples and the additional maxima seem to correlate to the form factor of the single Mo_{132} clusters: The second scattering maximum ($s = 0.14$ nm^{-1}) is caused by both the Mo_{132} clusters and the pore structure. There is no indication for the formation of any superstructure of Mo_{132} clusters within the silica mesopores. An additional hint for the origin of the scattering maxima in Figure 3b not belonging to the ordered silica is that after calcination (destruction of the Mo_{132} clusters) these patterns disappear. Nevertheless, the scattering pattern is also unusual because the lower order maxima of the Mo_{132} form factor are hardly visible, which we explain by the superposition with the mesopore form factor. It is also noticeable that the diffraction pattern at $s \approx 1$ nm^{-1} seems to be narrowed. At the moment we do not have any reasonable explanation for this observation.

The transformation of the Mo_{132} clusters to MoO_3 was performed by calcination in air for 2 h at 550 °C. During this process the color of the samples change from deep brown to colorless (white). Wide angle-X-ray scattering curves were recorded to monitor the transformation to MoO_3 (see Figure 3c). The scattering pattern is dominated by the broad diffraction pattern $2\theta = 0.39$ rad typical for amorphous silica. One relatively sharp signal at 0.47 rad and the broad signal 0.86 rad indicate the formation of MoO_3 in the pores. However, it is questionable from these measurements that the MoO_3 nanoparticles are fully crystalline. It even appears to be difficult to confirm the crystal phase and due to the silica backround very difficult to determine the crystal size via the diffraction width. Interestingly, in TEM (images not shown) the dark spots corresponding to Mo_{132} have disappeared and the porous silica matrix looks much more homogeneous. MoO_3 particles cannot be identified by TEM. A possible explanation for these findings could be that MoO_3 structures spread and cover the silica walls.

S_3 Materials. Materials were first characterized using sorption experiments. Results obtained for samples S_3 are very similar to those for samples S_2. The total

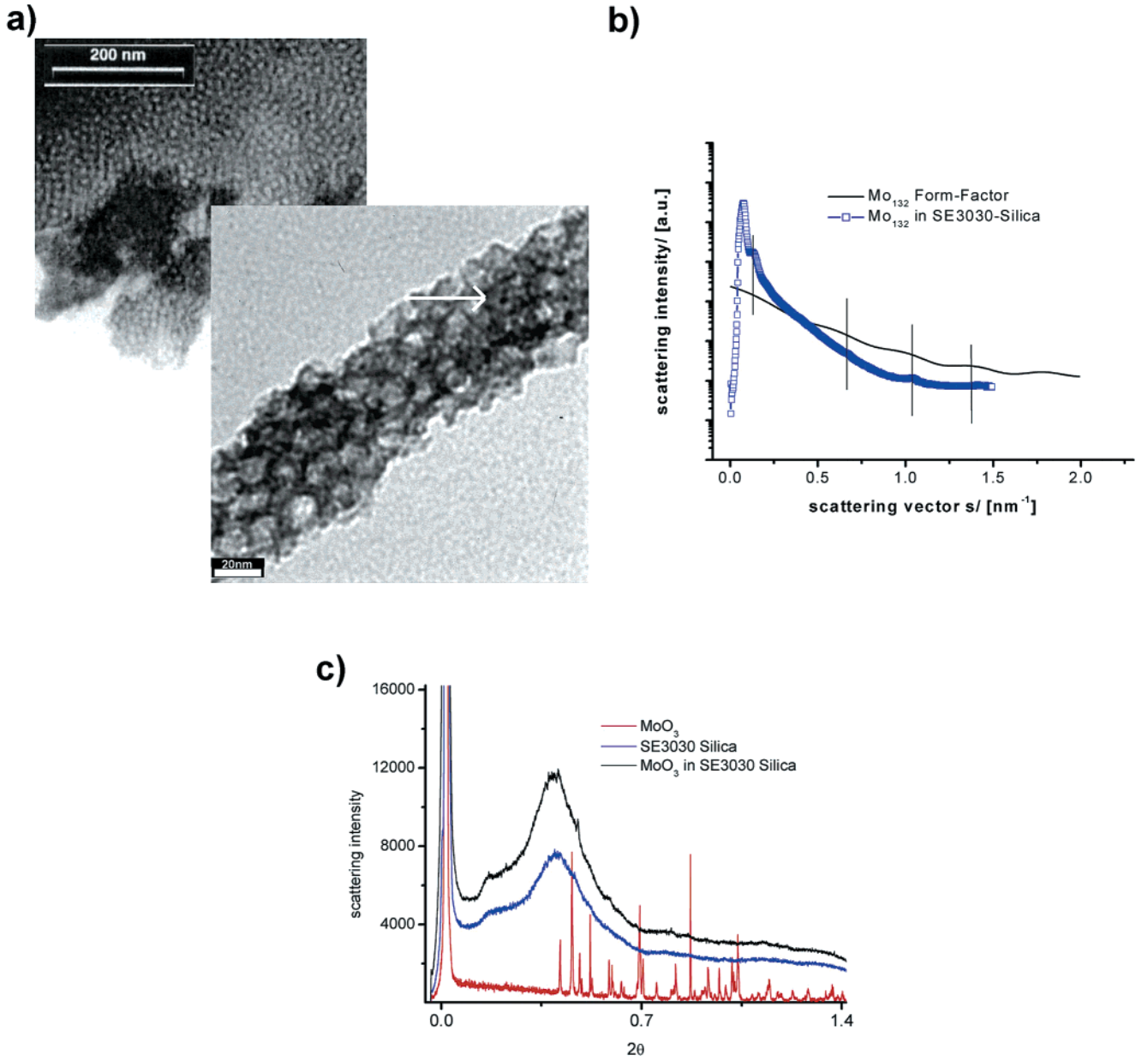

Figure 3. (a) shows two representative examples of ordered mesoporous silica materials (pore size ≈ 9.5 nm) with infiltrated supramolecular polyoxometalates of the Mueller type. Low magnifiactions are shown and the dark spots indicate higher electron density and hence the presence of molybdenum. (b) shows the small-angle X-ray pattern of the ordered mesoporous silica Mo_{132} composite and form factor of the Mo_{132} clusters determined by SAXS measurements on diluted solutions of Mo_{132} in water. The maxima of the form factor are marked to demonstrate the correlation. (c) shows WAXS patterns of crystalline MoO_3, pure silica, and the MoO_3−silica hybrid.

surface area has decreased slightly through the incorporation of the molybdenum oxide (from 550 to 400 m^2/g) but the whole mesopore volume is still accessible. Both isotherms of pure and MoO_3−silica are typical for mesoporous systems. The mesopores are not blocked, but partially filled with molybdenum oxide. The pore diameter of the pure SE_{3030}−silica decreases slightly (≈0.3 nm) for the MoO_3−silica hybrid materials. A decrease of the pore volume from 0.55 to 0.53 cm^3/g is observed. TEM measurements were performed on these MO−silica hybrid materials, but it was very difficult to evidence the presence of molybdenum oxide inside pores similar to the $S_{1/2}$ samples after calcination.

Infrared (IR) spectra were recorded in the 500−2500-cm^{-1} region for each type of MO−silica hybrid materials. It has to be mentioned that the SiO_2 network is itself IR-active and therefore absorption bands caused by the encapsulation of molybdenum oxide can hardly be distinguished from the backround due to the very low molar ratio of molybdenum oxide compared to silica. Nevertheless, as depicted in Figure 4 the MoO_3−silica hybrid material shows two additional IR bands at around 960 and 890 cm^{-1}. This indicates that Mo is octahedrally coordinated.[46]

An absorption band at around 960 cm^{-1} is characteristic for the terminal molybdenum oxygen double-bond stretching mode. The one observed at around 890 cm^{-1} is related to the antisymmetric stretching of Mo−O−Mo octahedra linkage. However, the absorption band

(46) Anvar, M.; Hogarth, C. A.; Theocharis, C. R. *J. Mater. Sci.* **1989**, *24*, 2387.

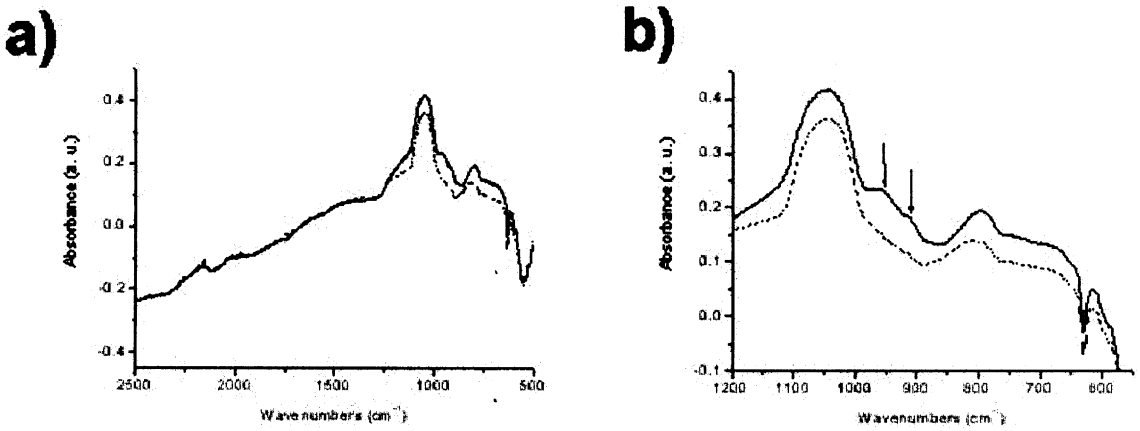

Figure 4. IR spectra: whole range (a) and zoom in the 600−1200-cm^{-1} region (b) of pure silica (dotted lines) and MO−silica hybrid material.

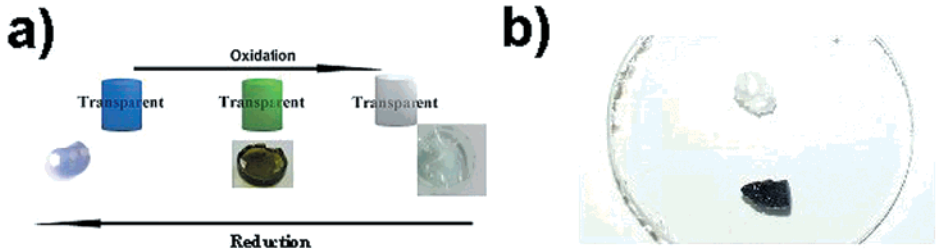

Figure 5. Photographic images of MO−silica hybrid materials S_1 (a) and S_3 (b) and their electrochromic behavior before, during, and after the redox process.

characteristic of the Mo−O at around a 640-cm^{-1} stretching mode was not observed in our spectra.[47,48]

It can be summarized that various forms of mesoporous silica can be filled with MoO_3 while maintaining high porosity, high access to the pores, and access to the MoO_3 species. Consequently, we have studied now chemistry with this nano-MoO_3 in pores and investigated the effect of the different pore environments.

Redox Chemistry of Molybdenum Oxide−Silica Hybrid Materials. Molydenum oxide and polyoxometalates are well-known electrochromic materials; the redox process has been mainly studied on powders or thin films.[49−51] Therefore, it is interesting to study if the present MoO_3−silica hybrid materials with their size-quantized structures show similar electrochromic responses.

The porous silica network provides diffusional pathways and access to the species encapsulated within the pores. It is thus possible to perform some chemical reactions directly inside pores, inside a confined environment. The reduction of the molybdenum oxide is performed chemically using hydrazinium sulfate [N_2H_6-(SO_4)] acting as a reducing agent. Samples were impregnated with the saturated solution of hydrazinium sulfate. For samples synthesized from route I (Figure 5a), a change of color from pale yellow via green to blue is observed and for samples from route II from colorless directly to blue as shown in Figure 5b. The reduction takes place only inside silica as no coloration of the external solution and no leaching was observed during the reaction. The $S_{2/3}$ samples exhibit immediate response (within a few seconds) while maximum coloration of the samples requires 1 h. Instead, S_1 samples need much more time to react, presumably due to the smaller transport pores (1.5 nm). The occurrence of the blue color can be attributed to a mixed-valence molybdenum oxide, well-known as molybdenum blue. Molybdenum blue species are referred to as compounds coming from redox processes resulting in a mixture of Mo(VI) and molybdenum in a lower oxidation state (Mo^V).

To study the change of oxidation state of molybdenum in more detail, in situ ESR measurements (at room temperature) were recorded every 15 min in the field region from 3000 to 4000 G, allowing the valence state of Mo to be followed. A ordered mesoporous silica containing no molybdenum was used as a reference. MoO_3−silica hybrid materials (S_1) were grinded in an agate mortar and then the resulting powder was placed inside a capillary, and a small amount of the hydrazin sulfate solution was added. After 30 min, a small signal centralized at around 3500 G is observed for sample containing molybdenum; its intensity increases with increasing time as shown in Figure 6 whereas for pure silica reference no signal was observed at all.

The signal observed is characteristic of the presence of molydenum in the +5 oxidation state; it saturates after 120 min, so the reaction is completed.[52,53] In a recent publication concerning the effect of Mo oxidation

(47) Li, C.; Xin, Q.; Wang, K. L.; Guo, X. *Appl. Spectrosc.* **1991**, *45*, 874.
(48) Kondo, J. N.; Iizuka, M.; Domen, K.; Wakabayashi, F. *Langmuir* **1997**, *13*, 747.
(49) Andreev, V. N.; Nikitin, S. E.; Klinov, V. A.; Kozrev, S. V.; Leshchev, D. V.; Shtel'makh, K. F. *Phys. Solid State* **2001**, *439*, 788.
(50) Lee, S. H.; Seong, M. J.; Tracy, C. E.; Mascarenhas, A.; Pitts, J. R.; Deh, S. K. *Solid State Ionics* **2002**, *147*, 129.
(51) Mestl, G.; Verbruggen, N. F. D.; Bosch, E.; Knozinger, H. *Langmuir* **1996**, *12*, 2961.
(52) Kucherov, A. V.; Slinkin, A. A. *Stud. Surf. Sci. Catal.* **1998**, *188*, 567.
(53) Kucherov, A. V.; Slinkin, A. A. *Catal. Lett.* **2000**, *64*, 53.

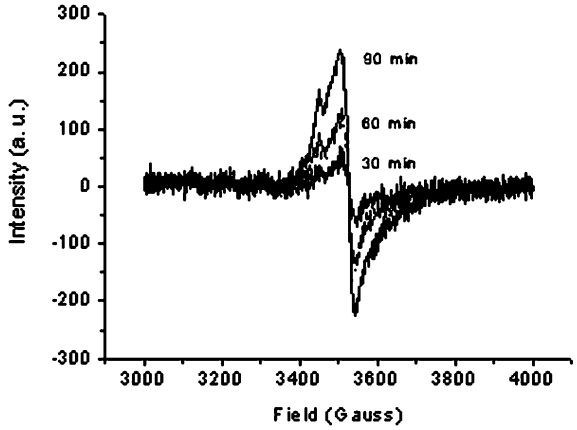

Figure 6. Time-dependent ESR spectra of S_1 samples.

states on the thermal coloration of amorphous MoO_3 films, it was demonstrated that the deep blue coloration observed was achieved without the contribution of Mo(IV). A statistical distribution of species with oxidation states of +5 and +6 was proved using X-ray photoelectron spectroscopy (XPS). Thus, in our samples, in agreement with results obtained using ESR, we can assign the blue color to the presence of a mixed Mo(V)−Mo(VI) oxide.[54] In comparison to the analogous bulk reduction, the process is slower in pores but no different reduction state than Mo^V is found.

To investigate in more detail the reduction/coloration process from a kinetic point of view, absorption measurements were performed on all samples. We employed diffuse reflection (DR) spectroscopy as a simple characterization tool. The DR spectra of the reduction process (in hydrazine sulfate solution) for all samples and pure silica for comparison were recorded. The spectrum for the pure silica and for all samples before reduction are very similar, showing constant reflection values over all the UV region mainly due to scattering. In contrast, the appearance of the spectrum (Figure 7a) of the samples after reduction is markedly different from that of pure silica and exhibited the appearance of a broad absorption band with maximum at 430 nm (~2.5 eV). This band can be attributed to the mixed valence Mo^{VI}/Mo^V molybdenum-blue species. Porter et al. observed the intervalence charge transfer (IVCT) bands at 2.13, 2.42, and 1.3 eV for Mo_4O_{11} and 2.48 eV for MoO_2. Thus, the degree of reduction determines the position of the absorption band.[55] It was also reported that molybdenum blue shows two bands, one at ~2.5 eV that was assigned as a d−d band for the Mo^{5+} center in a roughly C_{4v} site and a second one at ~1−1.65 eV that was assigned to the IVCT transitions between Mo^V and Mo^{VI} via an oxo-bridge.[56] The literature not being coherent, we can only say that a broad absorption band at around 430 nm (~2.5 eV) is a feature for the reduction of Mo^{VI} to Mo^V centers.

To study the reversibility of this redox process, absorption measurements were performed after five cycles of reduction−oxidation (Figure 7a). Oxidation was done using a concentrated solution of H_2O_2. For all samples, the same behavior was observed: A disappearance of the band at 430 nm after oxidation and coloration back to blue during reduction. There was no significant change in spectral properties after the cycles were performed. This clearly demonstrates that the redox process is fully reversible.

DR spectroscopy at a fixed wavelength was finally used to investigate the kinetics of the reduction process for all samples. The same amounts of powder and reduction solution were employed to compare the kinetics between samples. The evolution of the absorption at 430 nm as a function of time is shown in Figure 7b. For samples S_2 and S_3, the absorption increases rapidly during the first 20 min, and then it begins to saturate. After 50 min, the final absorption value is reached. The slope at small periods of time is very similar for both samples. However, sample S_3 seems to reach equilibrium in a longer time period (20 min more). For samples S_1, the increase in absorption value and therefore the reduction is much slower. Indeed, sample S_1 presents the smallest transport pores and thus it takes a longer time for the solution to reach them. The difference in absorption value at equilibrium can be due to a variety of reasons, for instance, by the different total number of molybdenum atoms encapsulated or by an altered mixed-oxide stoichiometry due to the different quantum confinements and size/shape of the molybdenum clusters involved. At this stage of the study it is not possible to differentiate between these possibilities. We evaluated the kinetics of the coloration process in further detail. Interestingly, sample S_1 with its smallest pore

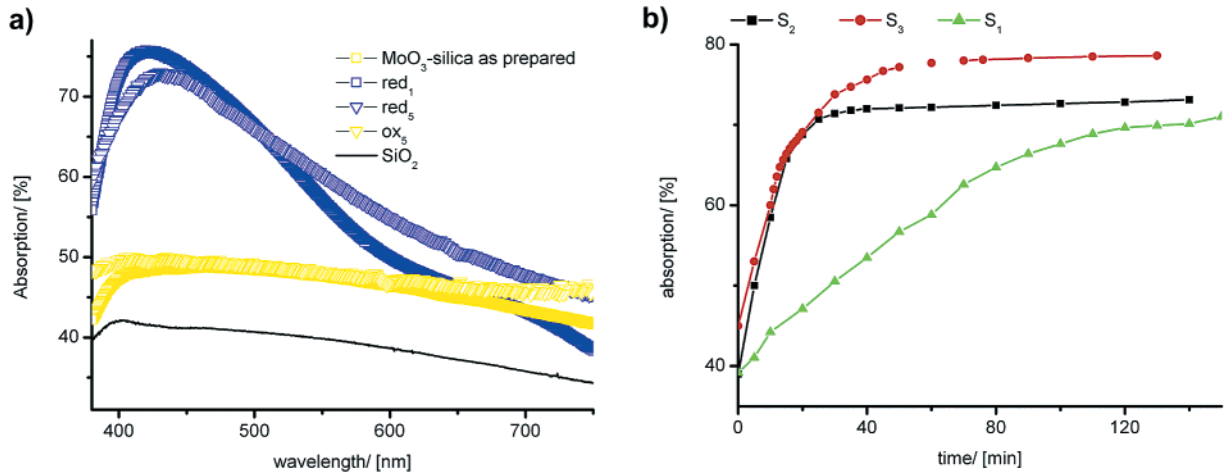

Figure 7. Absorption spectra of pure silica and MO−hybrid silica (S_3) before and after reduction (red_x = after x number of cycles) (a) and evolution of absorption as a function of time for MO−silica hybrid materials S_{1-3} (b).

size shows a first-order kinetics, as determined by a plot of ln $c(Mo^V)$ against t derived from the absorption spectra via Lambert−Beers law ($A \propto c$). The kinetics of S_2 and S_3 is more complex and is of higher order than 2. This result is very important because it shows that the kinetics of a process inside a pore can be controlled via pore size. In very small pores, first-order kinetics are enforced, although the "true" order of the reaction might be higher.

Conclusion

The encapsulation of different molybdenum oxide cluster species into mesoporous silica and their in situ reduction was described. As molybdenum oxide interacts only weakly with silica, it is usually very difficult to prepare molybdenum oxide supported on silica with high dispersion and uniform structure. The approach presented here solves this problem as the active species—molybdenum oxide clusters—are nanosized, their distribution inside the silica is uniform, and they are accessible to reactant molecules, being protected at the same time against major large-scale structural changes.

Different ways of synthesis and precursors leading to different MoO_3−silica hybrid materials were explored. Each route presents some specific advantages. In route I, where polyoxometalates act as templates and as precursors, the total number of molybdenum atoms in each confinement is known and kept throughout the reactions. In route II in which mesoporous silica is used as a starting material, it is possible to vary the total number of Mo atoms by repeating the impregnation process several times. This way of synthesis permits also one to envisage the encapsulation of various species at the same time.

Under reducing conditions, MoO_3−silica hybrid materials exhibit a change of color from white or slightly yellow to dark blue. This redox process is fully reversible. The blue color is due to the presence of a mixed valence molybdenum oxide (MoV/MoVI), as was confirmed by in situ ESR, IR spectroscopy, and absorption measurements.

It was not possible to give further details on the structure of the encapsulated molybdenum oxide, which are preferentially gained by EXAFS measurements at the Mo K-edge. These planned experiments will give information on the influence of confinement on the structure of the clusters. As shown by diffuse reflectance (DR) spectroscopy, these materials may be used as reversible redox sensors. The slow response of the materials prepared as grinded monoliths allowed us to follow and correlate the color to a distinct pair of oxidation states of Mo, the prerequisite for a reliable redox sensor.

It is expected that the time scale of the response of the materials could be significantly improved by the synthesis of the samples as thin films and further optimization of pore size/pore architecture. It was already shown that the smaller the pores are that access the MoO_3-containing pores, the slower the response of the materials.

Finally, these materials may also be interesting as oxidation catalysts as they fulfill several criteria characterizing a controlled or model catalyst.

Acknowledgment. The Max-Planck Society is acknowledged for financial support.

(54) Siokou, A.; Leftheriotis, G.; Papaefthimiou, S.; Yianoulis, P. *Surf. Sci.* **2001**, *482−485*, 294.
(55) Porter, V. R.; White, W. B.; Roy, R. *Solid State Chem.* **1972**, *4*, 250.
(56) Bugayev, A. A.; Nikitin, S. E. *Opt. Commun.* **2000**, *180*, 69.